

CRYSTAL STRUCTURE MODELING OF A HIGHLY DISORDERED POTASSIUM BIRNESSITE

KERRY L. HOLLAND† AND JEFFREY R. WALKER

Department of Geology and Geography, Vassar College, Poughkeepsie, New York 12601

Abstract—The structure of a highly disordered synthetic birnessite was studied by comparing powder X-ray diffraction (XRD) data with calculated patterns generated by BIRNDIF and WILDFIRE© in an attempt to describe the nature of disorder and to estimate the size of the coherent diffracting domains. The material has a turbostratic stacking sequence and coherent diffracting domains that are 25 to 30 Å on a side in the *ab* plane ($N_1 = 5$ unit cells, $N_2 = 10$ unit cells) and which average 2.5 unit cells thick parallel to *c*. Turbostratic stacking probably results because there are few constraints on the relationship between adjacent layers.

Key Words—Birnessite, Crystal Structure Modeling, Turbostratic Stacking.

INTRODUCTION

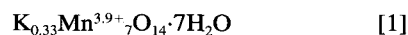
Birnessite is a phyllosilicate, one of a family of Mn-oxide minerals with similar layer structures and different interlayer arrangements, which includes chalcophanite with interlayer Zn, birnessite with a variety of interlayer cations, busserite with hydrated interlayer cations, asbolane with interlayer cations octahedrally coordinated by OH and vernadite (Burns and Burns 1976). These phyllosilicates are of interest in sedimentary environments because they can be effective scavengers and oxidizers of metals (Oscarson et al. 1981; Moore et al. 1990). Results of an investigation of the oxidation of arsenic by birnessite suggest that the crystal structure of the mineral is important to its efficient participation in this reaction (Moore et al. 1990).

However, due to their fine grain size and poor crystallinity the structures of the phyllosilicates are not well known. Most are seen as derivatives of the chalcophanite structure (Wadsley 1955), which is based on sheets of edge-sharing Mn^{4+} -O octahedra. In chalcophanite, vacancies in the Mn-O octahedra create charge deficiencies that are balanced by Zn cations in the interlayers (Post and Appleman 1988). Giovanoli et al. (1970) and Burns and Burns (1976) suggested that birnessite has a similar structure in which Mn atoms occupy the Zn sites; however, a recent refinement of the birnessite structure (Post and Veblen 1990) was unable to resolve whether layer charge resulted from substitution of Mn^{3+} for Mn^{4+} or from the presence of vacancies. Post and Veblen (1990) also reported asymmetric broadening of (*hk*0) peaks, which they felt did not affect their refined atomic coordinates but did suggest the presence of some degree of structural disorder.

Naturally-occurring birnessite is often very poorly crystalline with only a few broad diffraction peaks. Most careful crystal structure work has been conducted on synthetic specimens that have a reduced variety of interlayer cation species and, since they are relatively well-crystallized, exhibit sufficient diffraction maxima to make structural studies possible. The relationship between the poorly crystalline natural material and the relatively well-crystallized synthetic material is not clear. It is the aim of this work to investigate the crystal structure of a poorly crystalline synthetic K-birnessite that might be thought of as an analog for natural specimens.

EXPERIMENTAL METHODS

Samples of synthetic K-birnessite were obtained from J. N. Moore, at University of Montana. The material was synthesized by reduction of $KMnO_4$ with HCl. Details of synthesis and subsequent reaction experiments with As are given by Moore et al. (1990). The chemical composition of the samples at the time of synthesis was (Moore et al. 1990):



The cell parameters and atom positions of Post and Veblen (1990) were used in the structural modeling with the exception of *c*, which was calculated from the position of the (002) peak in the experimental diffraction pattern (Table 1).

XRD data were collected with a Siemens D5000 diffractometer using $CuK\alpha$ radiation (40 kV, 30 mA), a graphite monochromator, a 1°-divergence slit assembly and a 0.6-mm receiving slit. Samples were back-packed in an Al mount and scanned from 10 to 90 °2θ using a step of 0.05 °2θ. Between 10 and 55 °2θ, the samples were analyzed at 20 s/step and between 55 and 90 °2θ at 60 s/step. A representative diffraction pattern is shown in Figure 1a.

† Present address: Colorado School of Mines, Boulder, Colorado.

Table 1. K-birnessite atomic and cell parameters (Post and Veblen 1990).

	x	y	z	occ†	Temp factor
Mn	0	0	0	2	0.5
O	0.365	0	0.136	4	1
K	0.723	0	0.522	0.5	0.5
H ₂ O	0.723	0	0.522	0.5	1.5
O	0	0	0.5	0.3	1

$a = 5.149 \text{ \AA}$
 $b = 2.834 \text{ \AA}$
 $c = 7.176 \text{ \AA}$
 $\beta = 100.76^\circ$

† occ = occupancy factors in atoms/unit cell.

Diffraction results were modeled using 2 programs, both modifications of existing software. The first program, BIRNDIF, was modified from CLAYDIF (Reynolds 1985) by adding the X-ray scattering coefficients (Wright 1973) for Mn and by substituting the atomic coordinates of the birnessite Mn-O octahedral layer for one of the silicate layers in the program. BIRNDIF calculates the basal diffraction pattern of birnessite and

can be used to determine the mean defect-free stacking distance (δ) perpendicular to the layers by iterative modeling of selected basal peak shapes and widths.

The second program, WILDFIRE© (Reynolds 1993, 1994), was also modified to include X-ray scattering by Mn. Because WILDFIRE© uses an input file of atomic coordinates, it did not have to be modified to include the birnessite structure. The monoclinic coordinates of Post and Veblen (1990) were transformed to orthogonal space as described by Reynolds (1993) prior to modeling.

WILDFIRE© calculates diffraction phenomena from non-basal atom planes within the crystal. It performs the calculation by sweeping a vector $1/d$ in length through reciprocal space and calculating the contribution to diffracted intensity at each point on the resulting surface. Because layered minerals can exhibit varying amounts of disorder in one dimension (perpendicular to the layers), diffraction spots in reciprocal space are stretched parallel to the direction of the disorder (c^*) with maxima that vary in intensity depending upon the severity of the disorder and the change in the structure factor along c^* . For the maximum

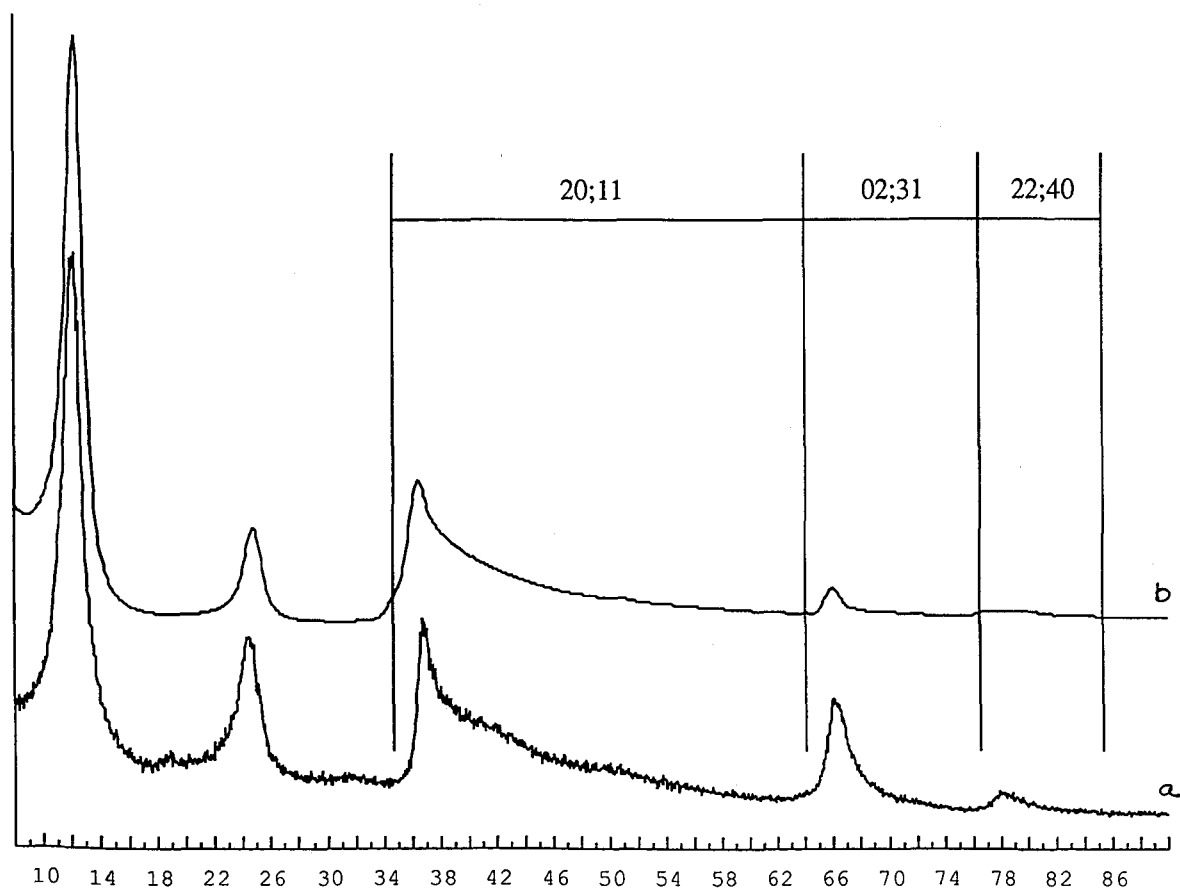


Figure 1. X-ray powder diffraction patterns of potassium birnessite identifying the 2-dimensional diffraction bands. 1a) Experimental data. 1b) Calculated pattern which is a combination of patterns calculated by BIRNDIF and WILDFIRE©.

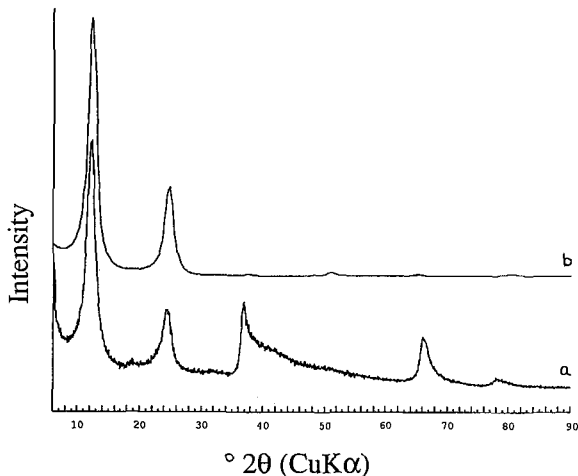


Figure 2. Comparison of calculated basal XRD pattern with experimental pattern. 2a) Experimental data (same as Figure 1a). 2b) Diffraction pattern calculated using BIRNDIF.

amount of disorder as represented by turbostratic stacking (that is, each layer is translated and/or rotated randomly in relation to adjacent layers), intensity varies smoothly along the axis of stretching and the spots become rodlike.

Variables that were manipulated during modeling with WILDFIRE© were the proportion of Mn to simulate vacancies or Mn^{3+} substitution, and the size of coherent scattering domains in terms of the number of unit cells along the $a = N1$, $b = N2$ and $c = N3$ axes in WILDFIRE©. The final calculated pattern (Figure 1b) was created by adding the basal diffraction pattern calculated by BIRNDIF to the non-basal pattern calculated by WILDFIRE© (Reynolds 1993) for reasons discussed below.

RESULTS

The diffraction pattern from the K-birnessite used in this study contains 5 broad peaks, 3 of which are asymmetric. Initial investigations of this sample (Moore et al. 1990) reported data to $65^\circ 2\theta$ (CuK α) and assumed that all peaks represented (00 l) diffraction. However, modeling of the diffraction pattern with BIRNDIF indicates that only the 001 and 002, and possibly the 004, peaks are present at the resolution of the experimental pattern (Figure 2). Therefore, other peaks in evidence must be due to hkl diffraction. BIRNDIF modeling also determined that the mean defect-free distance (δ) parallel to c is 2.5 unit cells.

The character of the asymmetry of the maxima at 35, 66 and $78^\circ 2\theta$ suggests that the layer stacking is turbostratic, in which case the asymmetric peaks represent the (20;11), (02;31) and (22;40) diffraction bands (Figure 1). To test this hypothesis, hk diffraction was modeled with WILDFIRE© by setting $N3 = 1$ unit cell (i.e., no coherence along the c axis). Best

results were obtained by setting $N1 = 5$ unit cells and $N2 = 10$ unit cells, suggesting that the diffracting domains are equidimensional in the ab plane with sides 25 to 30 Å in length.

DISCUSSION

The most important results of this study are the turbostratic nature of the layer stacking of this birnessite sample and the small size, but nearly equidimensional ab shape, of its diffracting domains. The nature of this disorder is consistent with the findings of Post and Veblen (1990), who reported streaking in (110) electron diffraction peaks and broadening of (111) XRD peaks.

Confusion may arise because the diffraction domains are said to be 2.5 unit cells along the c axis for (00 l) reflections yet only 1 unit cell thick for 3-dimensional reflections. The mean defect-free distance (δ) is the average number of parallel layers, so the reported distance implies that stacking sequences average only 2.5 layers without a stacking fault disrupting the parallelism of the layers. Rotations and translations of adjacent layers do not affect δ as long as they do not disrupt that parallelism; however, non-basal atom planes are not coherent across the interface and $N3 = 1$. Because WILDFIRE© cannot reconcile $\delta = 2.5$ and $N3 = 1$, the final calculated pattern is a composite of the 1-dimensional diffraction pattern calculated with BIRNDIF using the appropriate mean defect-free distance, and the 3-dimensional diffraction pattern calculated with WILDFIRE© using the appropriate $N3$.

Occurrence of turbostratic stacking sequences may be controlled by the nature of the basal atomic surface of the octahedral layers. The regular basal surface of the birnessite octahedral layers presented to the interlayer region is made up of O atoms with, possibly, some OH molecules. The regularity of this surface produces no holes into which large interlayer cations can fit. The situation is analogous to the smectites in which turbostratic stacking is common because the interlayer space is large enough to accommodate hydrated cations or molecules of ethylene glycol. Turbostratic sequences are not common in illite or micas where layers collapse around dehydrated interlayer cations that fit into the ditrigonal holes in the silicate layer base.

The fact that the atoms of the basal plane of birnessite are predominantly O rather than OH groups implies that H-bonding is not common although it is an important bonding mechanism in many other layered structures. Turbostratic stacking is rare in chlorite, for instance, where H bonds between interlayer OH groups and silicate basal O atoms are strong enough to be the only force joining the layers (Bish and Giese 1981).

Because sites of vacancies or Mn^{3+} in the octahedral layers appear to be disordered, the location of layer

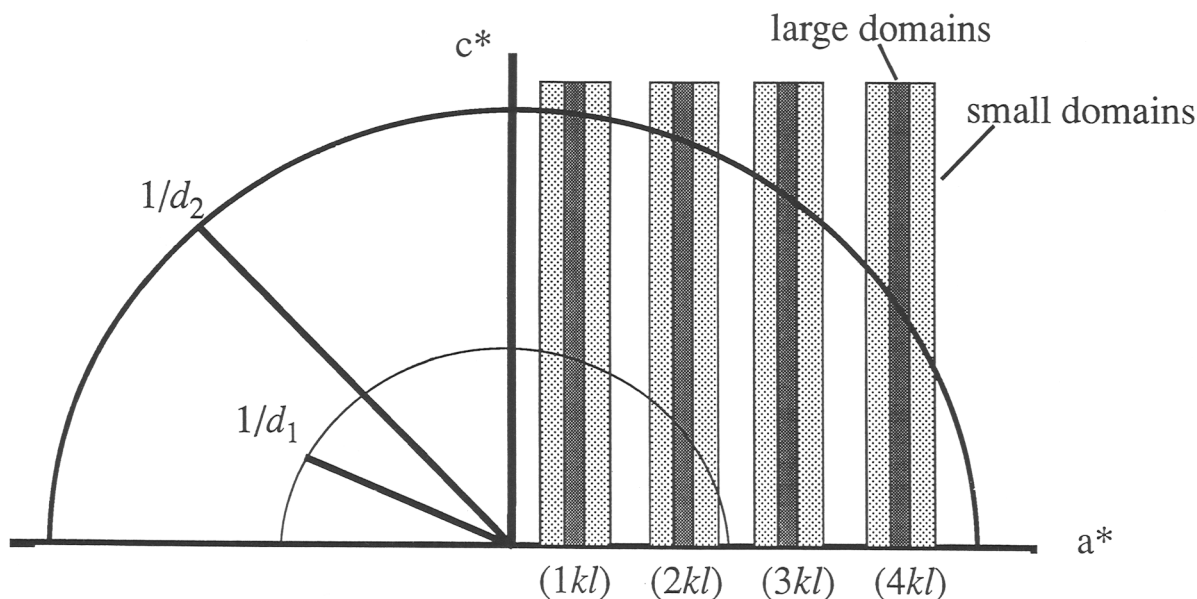


Figure 3. Schematic representation of the upper half of an a^*c^* reciprocal lattice plane demonstrating the method of calculation used by WILDFIRE© for a 2-dimensional crystal (Reynolds 1993). The vertical columns labeled $(1kl)$, $(2kl)$, etc., are reciprocal lattice rods of a turbostratic crystal. The structure factor varies smoothly along the rods. Vectors $(1/d_1, 1/d_2, \text{etc.})$ are swept through reciprocal space and a diffracted intensity is calculated wherever a vector intersects a rod. If diffracting domains are small, the diameter of the rods is large (lighter pattern) and the structure factor is more likely to change over the portion of the rod included in the calculation. In addition, rods of higher index, such as $(3kl)$ and $(4kl)$, are cut by the vector at a lower angle to their axes relative to rods of lower index, such as $(1kl)$ and $(2kl)$, so the area of the rod included by the calculation is larger, further increasing the chances that the structure factor will vary over the portion of the rod included.

charge associated with these charge deficiencies is also disordered. The K atoms in the interlayer of K-birnessite, which are in the same crystallographic sites as the H_2O molecules in the center of the interlayer (Post and Veblen 1990), can be coordinated by O atoms anywhere in the basal planes of the surrounding layers and are probably located near the disordered layer charge centers of the 2 adjacent octahedral layers in a configuration that maximizes local charge balance and minimizes cation repulsion.

The regularity of the atomic surface, the probable lack of H-bonding and the disorder of layer charge sites indicate that there are few constraints on the way in which successive octahedral layers articulate around the interlayer. These factors further suggest that Na-birnessite, in which Na atoms occupy the same crystallographic plane as the water molecules in K-birnessite (Post and Veblen 1990), should also form turbostratic stacking sequences, whereas Mg-birnessite, in which Mg cations are located between the H_2O layer and the basal O planes (Post and Veblen 1990), might form more ordered structures.

The agreement between the observed and calculated patterns in this study is not perfect, and becomes worse at higher diffraction angles. There are several possible reasons for this discrepancy. WILDFIRE© is optimized for the study of illite using diffraction phe-

nomena below approximately $45^\circ 2\theta$ ($\text{CuK}\alpha$). If the temperature factor (μ_{iso}) used is too large, calculated intensities will become increasingly smaller than experimental intensities at higher diffraction angles. However, even when μ_{iso} was decreased to $1/3$ of the default value, no significant improvement in the agreement of high angle intensities was noted.

WILDFIRE© is also optimized to model diffracting domains that are large in the ab plane (300 \AA on a side), making the assumption that the structure factor (F) is constant across the diffraction "rods" in reciprocal space (Reynolds 1993). As shown in Figure 3, this assumption may not be valid for diffracting domains that are as small as those modeled for this birnessite. For small diffracting domains, the diameter of the diffraction "rods" in reciprocal space is proportionately larger, increasing the possibility that F is not constant in the region of the calculation. Additionally, at increasingly higher indices, the diameter ($1/d$) of the hemisphere over which intensity is integrated becomes larger, so the calculation sweeps through the rod at a lower angle to the axis of the rod and incorporates a larger portion of reciprocal space. Because intensity varies smoothly along the rods, there is a greater chance that the structure factor will change in the calculation region. The 2 higher angle diffraction bands contain diffraction phenomena from the $(31l)$ and $(40l)$

classes of reflections, respectively, and so may be affected by changes in the structure factor across the (31) and (40) diffraction rods.

It was not possible with the data and analytical method used here to distinguish between the 2 possible layer-charge producing mechanisms, vacancies or Mn^{3+} substitution. The samples used in this study were prepared under reducing conditions so some Mn^{3+} may be present in the octahedral layers. The proportion of vacancies or trivalent substitution is small (Post and Veblen 1990) and their presence is probably not recognizable given the structural disorder evidenced by the data. It has been noted that birnessite prepared under oxidizing conditions tends to form more well-ordered crystals than that prepared under reducing conditions (Alain Manceau, personal communication, 1994) suggesting that future studies might address the structural differences between birnessites synthesized by the 2 different methods.

CONCLUSION

Although the birnessite studied here is synthetic, it has an XRD pattern that suggests crystalline disorder analogous to that found in naturally-occurring samples. The mineral has a turbostratic stacking sequence and coherent diffracting domains that are 25 to 30 Å on a side in the *ab* plane and average 2.5 unit cells thick parallel to *c*. Turbostratic stacking probably results because there are few constraints on the articulation of adjacent layers. The experimental and calculated XRD patterns are not in perfect agreement, especially at higher diffraction angles, possibly because the assumption made by WILDFIRE© that the structure factor does not vary across the diffraction "rods" in reciprocal space may not be valid for such small diffracting domains and/or reflections with such high indices.

ACKNOWLEDGMENTS

We would like to thank J. N. Moore for introducing us to birnessite and for providing us with these samples. The manu-

script benefited from reviews by R. C. Reynolds, Jr, J. E. Post and D. L. Bish. Address for A. Manceau personal communication: LGIT-IRIGW, BP53X, Grenoble 38041, France.

REFERENCES

- Bish DL, Giese R. 1981. Interlayer bonding in *IIB* chlorite. *Am Mineral* 66:1216–1220.
- Burns RG, Burns VM. 1976. Mineralogy of ferromanganese nodules. In: GP Glasby, editor. Marine manganese deposits. Amsterdam: Elsevier Science 554 p.
- Giovanoli R, Stähl E, Feitknecht W. 1970. Über Oxihydroxides des vierwertigen Mangans mit Schichtengitter, 1. Mitteilung: Natriummangan(II,III)manganat(IV). *Helv Chim Acta* 53:209–220.
- Moore JN, Walker JR, Hayes TH. 1990. Reaction scheme for the oxidation of As(III) to As(V) by birnessite. *Clays Clay Miner* 38:549–555.
- Oscarson DW, Huang PM, Liaw WK. 1981. The role of manganese in the oxidation of arsenite by freshwater lake sediments. *Clays Clay Miner* 29:219–225.
- Post JE, Appleman DE. 1988. Chalcophanite, $ZnMn_3O_7 \cdot 3H_2O$: New crystal-structure determinations. *Am Mineral* 73:1401–1404.
- Post JE, Veblen DR. 1990. Crystal structure determinations of synthetic sodium, magnesium, and potassium birnessite using TEM and the Rietveld method. *Am Mineral* 75:477–489.
- Reynolds RC, Jr. 1985. CLAYDIF: A computer program for the calculation of one-dimensional diffraction patterns of pure clay minerals. Hanover, NH: RC Reynolds, Jr, 8 Brook Rd.
- Reynolds RC, Jr. 1993. Three-dimensional X-ray powder diffraction from disordered illite: simulation and interpretation of the diffraction patterns. In: Reynolds RC, Jr, Walker JR, editors. CMS workshop lectures, vol 5, Computer applications to X-ray powder diffraction analysis of clay minerals. Boulder, CO: The Clay Minerals Society. p 43–78.
- Reynolds RC, Jr. 1994. WILDFIRE©: A computer program for the calculation of three-dimensional X-ray diffraction patterns for mica polytypes and their disordered variations. Hanover, NH: RC Reynolds, Jr, 8 Brook Rd.
- Wadsley AD. 1955. The crystal structure of chalcophanite, $ZnMn_3O_7 \cdot 3H_2O$. *Acta Crystallogr* 8:165–172.
- Wright AC. 1973. A compact representation for atomic scattering factors. *Clays Clay Miner* 21:489–490.

(Received 26 January 1994; accepted 23 January 1996; Ms. 2460)